Frozen mode regime in finite periodic structures

Huanan Li, Ilya Vitebskiy, and Tsampikos Kottos

Frozen Mode Regime in Finite Periodic Structures

Huanan Li,[1] Ilya Vitebskiy,[2] and Tsampikos Kottos[1, 3]

[1] *Department of Physics, Wesleyan University, Middletown CT-06459, USA*
[2] *Air Force Research Laboratory, Sensors Directorate,*
Wright-Patterson Air Force Base, OH- 45433, USA
[3] *KBRwyle, Dayton, OH 45431*

Periodic structures with Bloch dispersion relation supporting a stationary inflection point (SIP) can display a unique scattering feature, the frozen mode regime (FMR). The FMR is much more robust than common cavity resonances; it is much less sensitive to the boundary conditions, structural imperfections, and losses. Using perturbation theory, we analyze the FMR in the realistic case of a finite fragment of a periodic structure. We show that in close proximity of SIP frequency, the character of the FMR is qualitatively different from the known case of a semi-infinite structure.

Introduction –The ability to engineer composite structures with predefined wave dispersion is extremely important in acoustics and electrodynamics[1,2]. An outgrowth of this development was the realization of photonic structures which are now routinely used to control light propagation, as well as to modify all kinds of light-matter interactions. An important example is the possibility to drastically reduce the wave group velocity $v_g = \partial\omega/\partial k$ in periodic photonic structures, which is widely used for miniaturization and the enhancement of light-matter interaction. There are many ways to achieve a vanishingly small v_g. An obvious example is a photonic band edge, where the Bloch dispersion relation can be approximated as $\omega(k) - \omega_0 \propto (k - k_0)^2$. Another type of slow wave is associated with a stationary inflection point (SIP), where the Bloch dispersion relation has the form $\omega(k) - \omega_0 \propto (k - k_0)^3$. A SIP is associated with the frozen mode regime (FMR)[3,4] characterized by nearly total conversion of an input light into a slow (frozen) mode with dramatically enhanced amplitude. The FMR is not a resonance; unlike common Fabry-Perot (cavity) resonances, the FMR is not particularly sensitive to the size of the photonic structure and the boundary conditions. The FMR can tolerate much stronger losses and structural imperfections than any known cavity resonance. Finally, in a combination with non-reciprocity, the FMR can lead to the phenomenon of electromagnetic unidirectionality[5] which, in the presence of gain, can result in a cavity-less unidirectional lasing[6]. Due to the underlying mathematical complexity, the FMR has been fully analyzed only in semi-infinite periodic multilayered structures[7–9] and multimode waveguide arrays[10–12].

Here we are investigating the scattering problem for a finite multi-mode structure, whose periodic counterpart display SIPs. Using an abstract transfer matrix (TM) formalism together with a matrix perturbation approach, we studied the transmission characteristics of such set-ups in the FMR. We derived theoretical expressions for the energy flux carried by the slow propagating mode(s) and identify a new scaling behavior with respect to the frequency detuning. Specifically, we find that the energy fluxes, associated with the slow propagating mode(s), undergoes a transition at critical sample
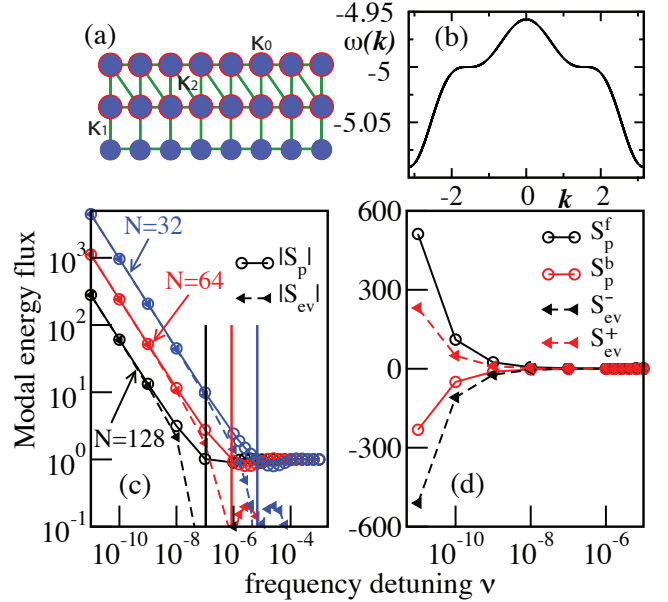
FIG. 1. (a) Schematic of the tight-binding model. The couplings $\kappa_{1,2} = 5$ and the on-site potential $\kappa_0 = 5$ are indicated in the figure. (b) A pair of symmetric SIP at $\omega(\pm k_0 = \pm\pi/2) = -5$. (c) The absolute value of the normalized (to the net flux) modal energy flux for the total propagating $|S_p| = |S_p^f + S_p^b|$ and the two pairs of evanescent $|S_{ev}| = |S_{ev}^- + S_{ev}^+|$ modes versus ν for three different sample lengths $N_1 = 32, N_2 = 64, N_3 = 128$. Vertical solid lines indicate $\nu_C \propto 1/N_C^3$, see Eq. (8). (d) The normalized modal energy fluxes (linear scale) associated with each of the propagating $S_p^{f/b}$ and pair of evanescent $S_{ev}^{\mp}$ modes for $N = 128$. The super- indeces $\mp$ in S_{ev} indicate that the corresponding pair is associated with the $T^{\mp}$ blocks (see Eq. (2)).

lengths $L_C \propto |\omega - \omega_{SIP}|^{-1/3}$ from an $S_p \sim \mathcal{O}(1)$ behavior (characteristic of semi-infinite structures) to an $S_p \propto |\omega - \omega_{SIP}|^{-2/3}$ law. The latter divergence is balanced by a simultaneous development of an energy flux carried by pairs of evanescent modes.

Transfer Matrix Formalism near SIPs– We consider (finite) periodic composite structures whose infinite counterpart has a dispersion relation $\omega(k)$ which supports

a SIP at some frequency ω_{SIP}. In the absence of any non-reciprocal elements, the dispersion relation is reciprocal $\omega(k) = \omega(-k)$ and therefore an ω_{SIP} is associated with two counter-propagating slow modes at $\pm k_{\text{SIP}}$. In such structures, two sets of three modes are responsible for SIPs at $\pm k_{\text{SIP}}$.

The wave propagation is analyzed using the TM approach. The TM $\mathcal{T}(z, z_0; \omega)$ connects the wave amplitudes (in mode space– see Ref.[13] for a coupled mode theory implementation) Ψ of a monochromatic wave at two different positions z and z_0 through the relation $\Psi(z) = \mathcal{T}(z, z_0; \omega)\Psi(z_0)$. For the specific case of periodic structures, the TM of a unit cell $\mathcal{T}(\nu) \equiv \mathcal{T}(1, 0; \omega_0 + \nu)$ dictates the transport. Here we assumed that the length of the unit cell is $L_{\text{uc}} = 1$, $\omega_0 = \omega_{\text{SIP}}$ and ν is the frequency detuning.

We consider a minimal model for which the unit TM $\mathcal{T}(\nu)$ is 6×6 and it is analytic around the SIP. Since a symmetric spectrum develops two SIPs at $\nu = 0$, $\mathcal{T}(0)$ can be represented by its Jordan normal form as

$$\mathcal{T}(0) = g_0(0)\begin{pmatrix} J^- & 0 \\ 0 & J^+ \end{pmatrix} g_0^{-1}(0); \, J^\pm \equiv e^{\pm \imath k_0}\begin{pmatrix} 1 & 1 & \\ & 1 & 1 \\ & & 1 \end{pmatrix}, \tag{1}$$

where $g_0(0) = [j_0^-, j_1^-, j_2^-, j_0^+, j_1^+, j_2^+]$ is an invertible 6×6 matrix with columns given by the Jordan basis vectors and $\pm k_0 = \pm k_{\text{SIP}}$. When $\nu \neq 0$ (but still $\nu \to 0$), $\mathcal{T}(\nu)$ reduces to its normal form[3,14,15]

$$g_0(\nu)^{-1}\mathcal{T}(\nu)g_0(\nu) = \begin{pmatrix} T^-(\nu) & 0 \\ 0 & T^+(\nu) \end{pmatrix}, \tag{2}$$

where $T^\pm(\nu) = J^\pm + T_1^\pm \nu + \cdots \equiv e^{\pm \imath k_0}(I_3 + Z^\pm(\nu))$ and the matrix $g_0(\nu)$ depends analytically on ν in the vicinity of $\nu = 0$.

Next we focus on the eigenvalue problem associated with the individual blocks of the normal form Eq. (2). Let us consider, for example, the block matrix $T^-(\nu)$ or its equivalent problem associated with the matrix $Z^-(\nu)$. Simple-minded normal perturbation theory is not useful in cases like ours when the leading term of the operation expansion is nilpotent i.e. $(Z^-(0))^3 = 0$. Indeed in such cases the standard Taylor series assumed for the eigenvalues is not the appropriate expansion; rather one has to develop the eigenvalue perturbation expansion using a Puiseux series[14,15]. Nevertheless, a singular perturbation theory provides a recipe to "reconstruct" the appropriate operator expansion after identifying the correct leading order term[15]. Using this approach we have found that $Z^-(\nu) = Z_0^-(\tilde{\nu}) + Z_1^- \tilde{\nu} + \cdots$ where $Z_0^-(\tilde{\nu}) \equiv \begin{pmatrix} 0 & 1 & 0 \\ 0 & 0 & 1 \\ 0 & 0 & 0 \end{pmatrix} + \tilde{\nu}\begin{pmatrix} 0 & 0 & 0 \\ 0 & 0 & 0 \\ 1 & 0 & 0 \end{pmatrix}$ and $\tilde{\nu} \equiv [Z^-(\nu)]_{31} = -\imath \frac{3!}{\omega'''(-k_0)}\nu + \mathcal{O}(\nu^2)$.

The diagonalization of $Z_0^-(\tilde{\nu})$, gives

$$G_0^{-1}(\tilde{\nu})Z_0^-(\tilde{\nu})G_0(\tilde{\nu}) = \tilde{\nu}^{1/3}\Lambda_0; \, \Lambda_0 = \text{diag}(c_0, c_1, c_2), \tag{3}$$

where $c_n \equiv e^{\imath \frac{2\pi}{3}n}$ and the similarity transformation matrix $G_0(\tilde{\nu})$ is a Vandermonde matrix[16] of order 3. Further, the diagonalization process for $Z^-(\tilde{\nu})$ (or equivalently $T^-(\nu)$) can be continued order-by-order, leading to the following compact form

$$e^{-S}G_0(\tilde{\nu})^{-1}T^-(\nu)G_0(\tilde{\nu})e^S$$
$$= e^{-\imath k_0}\left(I_3 + \tilde{\nu}^{1/3}\Lambda_0 + \tilde{\nu}^{2/3}\Lambda_1 + \cdots\right), \tag{4}$$

where the matrix $S \equiv S(\tilde{\nu}^{1/3}) = \tilde{\nu}^{1/3}S_1 + \tilde{\nu}^{2/3}S_2 + \cdots$ and $\Lambda_1, \cdots$ are diagonal matrices. A similar treatment applies for the eigenvalue problem associated with $T^+(\nu)$.

This approach allows us to evaluate perturbatively the eigenvalues $\theta_n^\mp(\nu)$ and the eigenvectors $f_n^\mp(\nu)$ of the unit TM $\mathcal{T}(\nu)$. We get

$$\mathcal{T}(\nu)f_n^\mp(\nu) = \theta_n^\mp(\nu)f_n^\mp(\nu), \, n = 0, 1, 2 \tag{5}$$
$$\theta_n^\mp(\nu) \approx e^{\imath(\mp k_0 + \lambda_n^\mp)}; \, \lambda_n^\mp(\nu) \equiv \alpha_0^\mp c_n \nu^{1/3}$$
$$f_n^\mp(\nu) \approx \left[1 - \imath \sigma_2^\mp \lambda_n^\mp + \eta^\mp(\lambda_n^\mp)^2\right]j_0^\mp$$
$$+ \left[\imath \lambda_n^\mp - \sigma_1^\mp(\lambda_n^\mp)^2\right]j_1^\mp - (\lambda_n^\mp)^2 j_2^\mp$$

where $\alpha_0^\mp = \left(3!/\omega'''(\mp k_0)\right)^{1/3}$, $\eta^\mp = \gamma_3^\mp - \gamma_1^\mp + \frac{1}{2}\left((\sigma_1^\mp)^2 + \sigma_1^\mp \sigma_2^\mp - (\sigma_2^\mp)^2\right)$, $\sigma_l^\mp = \frac{1}{3}\frac{[T_1^\mp]_{l+1,l}}{[T_1^\mp]_{31}}$, $\gamma_l^\mp = \frac{1}{3}\frac{[T_1^\mp]_{l,l}}{[T_1^\mp]_{31}}$ and $j_n^\mp$ is the Jordan basis of $\mathcal{T}(0)$.

We assume that $\nu \to 0^+$ and that the incident wave is entering the finite structure from the left interface at $z = 0$; for an example see the dispersion relation in Fig. 1b. We can now decompose any wave inside the structure to the forward (backward) propagating $f_0^-(f_0^+)$ and evanescent $f_1^-, f_2^+(f_1^+, f_2^-)$ modes and thus evaluate the associated conversion coefficients. We shall also analyze the energy flux carried from these modes and determine their scaling with respect to detuning ν.

Conversion Coefficients – We consider that the finite structure consists of N periods of the unit cell. In contrast to the semi-infinite case[3,10], finite structures involve two interfaces at $z = 0$ and $z = N$ and therefore both forward and backward modes can participate in the scattering process. When $\nu \to 0^+$, the eigenmodes Eq. (5) associated with different blocks in Eq. (2) become degenerate within the specific block. This observation forces us to construct a new "well-behaved" basis $\mathcal{B}_{fb} = \left\{f_0^-, \tilde{f}_1^-, \tilde{f}_2^-, f_0^+, \tilde{f}_1^+, \tilde{f}_2^+\right\}$, where the new basis vectors $\tilde{f}_1^\mp = \frac{f_1^\mp - f_0^\mp}{\imath \alpha_0^\mp \nu^{1/3}(c_1 - 1)}$ and $\tilde{f}_2^\mp = -\frac{1}{3(\alpha_0^\mp)^2 \nu^{2/3}}\left(c_2 f_2^\mp + c_1 f_1^\mp + f_0^\mp\right)$ together with $f_0^\pm$, are independent in the limit of $\nu \to 0^+$.

Next we couple semi-infinite leads to the left and right of the structure. We assume that the leads do not develop any spectral singularity around ω_0. We then request continuity of $\Psi(z)$ at the interfaces at $z = 0, N$ together with the scattering condition that the incident wave enters the

structure from the left i.e. that the coefficients of the backward modes on the right leads are zero. Finally the identification of the appropriate (non-degenerate in the $\nu \to 0$ limit) basis guarantee that the scattering problem has unique solution and that the expansion coefficients $\{\varphi_1^+, \varphi_2^+, \varphi_3^-, \varphi_1^-, \varphi_2^-, \varphi_3^+\}$ of $\Psi(z = 0^+)$ in the basis $\mathcal{B}_{fb}$ exists for any incident wave.

Obviously the specific values of the expansion coefficients depend on the particular form of the incident wave. Nevertheless some features are independent of the incident waveform; we find, for example, that $\varphi_l^\pm(\nu) = \varphi_l^\pm(0) + \mathcal{O}(\nu^{1/3})$ while the envelopes scale as $|\varphi_3^\pm(0)| \sim \mathcal{O}(N^{-1})$ and $|\varphi_j^\pm(0)| \sim \mathcal{O}(N^0)$, $j = 1, 2$, in the large N limit. Correspondingly, in terms of the eigenmodes of $\mathcal{T}(\nu)$, the expansion of $\Psi(z = 0^+)$ is given as

$$\Psi(z = 0^+) = \sum_{\sigma=\pm} \left[\frac{-\varphi_3^{-\sigma}}{3(\lambda_0^{-\sigma})^2} + \frac{-\varphi_2^\sigma}{\iota(c_1-1)\lambda_0^{-\sigma}} + \varphi_1^\sigma \right] f_0^{-\sigma}$$
$$+ \left[\frac{-c_1\varphi_3^{-\sigma}}{3(\lambda_0^{-\sigma})^2} + \frac{\varphi_2^\sigma}{\iota(c_1-1)\lambda_0^{-\sigma}} \right] f_1^{-\sigma} + \left[\frac{-c_2\varphi_3^\sigma}{3(\lambda_0^\sigma)^2} \right] f_2^\sigma, \quad (6)$$

where $\sigma = +/-$ correspond to forward/backward modes. Substitution of the scaling expressions for the expansion coefficients $\varphi_l^\pm$ together with $\lambda_0^{-\sigma}$ (see Eq. (5)) in Eq. (6), allow us to estimate the scaling of the conversion coefficients. Specifically we find that each of the square bracket terms in Eq. (6) scale as

$$[\cdots] \xrightarrow{\nu \to 0} \beta_2/(N\nu^{2/3}) + \beta_1/\nu^{1/3}; \quad (7)$$

where $\beta_{1,2}$ are some constants independent of N and ν. Equation (7) signifies a scaling transition from $1/\nu^{2/3}$ (small samples) to $1/\nu^{1/3}$ (large samples) at some critical sample length

$$L_C = L_{uc}N_C \propto L_{uc}/\nu^{1/3}. \quad (8)$$

While the latter scaling law for the conversion coefficients is already known from the case of semi-infinite structures, the former one is completely new and a trademark of the finite length nature of the scattering setting.

Modal energy flux – We now turn our focus on the consequences of the scaling (7) in the modal energy flux. First we recall that near a SIP the Bloch dispersion relation takes the form $\omega - \omega_0 \propto (k - k_0)^3$. The group velocity of the slow propagating mode(s) is

$$v_g = \frac{\partial\omega}{\partial k} \propto (k - k_0)^2 \propto (\omega - \omega_0)^{2/3} \quad (9)$$

while the associated energy flux contribution S_p is

$$S_p = W_p v_g \propto W_p \nu^{2/3} \quad (10)$$

where W_p is the energy density of the slow propagating mode. An estimation for the scaling of W_p is provided from the behavior of the conversion coefficients associated with $f_0^\pm$, see Eqs. (6,7), i.e. $W_p \propto |\beta_2/N\nu^{2/3} + \beta_1/\nu^{1/3}|^2$. In other words, W_p undergoes a

transition from an $1/\nu^{4/3}$ (for $N < N_C$) to an $1/\nu^{2/3}$ (for $N > N_C$) scaling with respect to the detuning ν.

In the latter limit of "semi-infinite" samples the sole contribution to the energy flux comes from the slow mode and thus $S = S_p = W_p v_g \sim \mathcal{O}(1)$, as expected also from previous studies[3,10] (see[17]). In contrast, in finite scattering set-ups, the contribution S_p from the slow propagating mode(s) to the total energy flux S is

$$S_p = W_p v_g \propto W_p \nu^{2/3} \propto \nu^{-2/3} \quad (11)$$

where we have used Eq. (10) together with the scaling behavior of W_p for short samples.

The anomalous scaling Eq. (11) of the modal energy flux of the propagating modes near the SIP can be balanced only by the same type (but different in sign) of divergence of modal energy flux S_{ev} carried by the two pairs of forward and backward evanescent modes. This is necessary in order to get a total energy flux $S \sim \mathcal{O}(1)$ and it is a new feature associated with the fact that the scattering set-up is finite. Below we will check these predictions using some simple numerical examples.

Tight-binding model – We first consider a tight-binding (TB) model supporting a symmetric dispersion relation with two SIPs, see Fig. 1a,b. This system can be realized as a quasi-one-dimensional array of coupled resonators[18–20]. The system consists of $M = 3$ chains of coupled resonators where the resonators of each chain have equal nearest-neighbor coupling (set to be 1 as coupling unit). The vertical inter-chain coupling between the nearest chains is κ_1. In addition, the resonators at the first two chains have an on-site potential contrast κ_0 (with respect to the resonators of the third chain) and they are also coupled via an inter-chain diagonal coupling κ_2. In this TB model a monochromatic wave is described by

$$\omega E_l^{(1)} = E_{l-1}^{(1)} + E_{l+1}^{(1)} + \kappa_1 E_l^{(2)} + \kappa_2 E_{l+1}^{(2)} + \kappa_0 E_l^{(1)}$$
$$\omega E_l^{(2)} = E_{l-1}^{(2)} + E_{l+1}^{(2)} + \kappa_1 \left(E_l^{(1)} + E_l^{(3)} \right) + \kappa_2 E_{l-1}^{(1)} + \kappa_0 E_l^{(2)}$$
$$\omega E_l^{(3)} = E_{l-1}^{(3)} + E_{l+1}^{(3)} + \kappa_1 E_l^{(2)}, \quad (12)$$

where $E_l^{(m)}$ is the field amplitude at the site l of the chain m. Substituting $E_l^{(m)} = A^{(m)} e^{\iota k l}$ in Eq. (12), we get

$$\omega u_A = D u_A; \quad D \equiv \begin{pmatrix} \epsilon(k) & v(k) & 0 \\ v^*(k) & \epsilon(k) & \kappa_1 \\ 0 & \kappa_1 & 2\cos k \end{pmatrix} \quad (13)$$

where $\epsilon(k) = 2\cos k + \kappa_0$, $v(k) = \kappa_1 + \kappa_2 e^{\iota k}$ and $u_A = \left(A^{(1)}, A^{(2)}, A^{(3)} \right)^T$. Then the dispersion relation $\omega(k)$ is obtained by setting $\det(D - \omega I_3) = 0$. Generally there are three bands for this model and we mainly focus on the band supporting SIPs characterized by $\omega'(\pm k_0) = \omega''(\pm k_0) = 0$ and $\omega'''(\pm k_0) \neq 0$. An example is given in Fig. 1b, where for the parameter values $\kappa_0 = \kappa_1 = \kappa_2 = 5$ and SIPs at $\pm k_0 = \pm\frac{\pi}{2}$ and $\omega_0 = -5$.
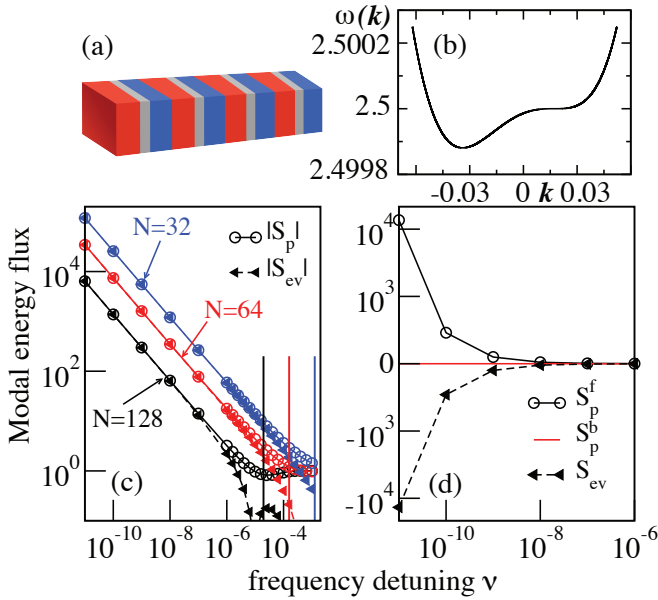
FIG. 2. (a) A multilayered photonic structure with $\omega(k) \neq \omega(-k)$[17]. (b) The dispersion relation of the structure supports one SIP with one forward slow propagating and two evanescent modes. (c) Scaling of modal energy flux for the (sum of) propagating $|S_p| = |S_p^f + S_p^b|$ and the pair of evanescent $|S_{ev}|$ modes versus the frequency detuning ν for three different sample lengths $N_1 = 32, N_2 = 64, N_3 = 128$. Vertical lines indicate the scaling law Eq. (8) (d) The modal energy fluxes associated with each of the propagating $S_p^{f/b}$ and pair of evanescent S_{ev}^- modes for $N = 128$.

The scattering sample is attached to the left and to the right with semi-infinite leads, which are composed of three decoupled chains with constant nearest-neighbor coupling κ_L in each chain. Thus the leads support a traveling wave whenever its frequency is within the band $\omega(k_L) = 2\kappa_L \cos k_L$ where $-\pi \leq k_L < \pi$. The field amplitude in each lead-chain can be written as a sum of two counter-propagating waves, *i.e.*, $E_l^{(m)} = a^{(m)} e^{\imath |k_L| l} + b^{(m)} e^{-\imath |k_L| l}$. In the simulations, we assume $\kappa_L = 4$ so that $b^{(m)}$ represents the amplitude of incoming waves since $v_g \equiv \frac{\partial \omega}{\partial k_L} \big|_{-|k_L|} > 0$.

Finally the energy flux through a section l in the scattering domain is defined using the continuity equation,

$$\frac{d}{dt}\left[\sum_m E_l^{(m)*} E_l^{(m)}\right] = F_{l-1\to l} - F_{l\to l+1} \qquad (14)$$

where $F_{l-1\to l} \equiv 2\mathcal{I}m\left[\sum_m E_{l-1}^{(m)} E_l^{(m)*} + E_{l-1}^{(1)} \kappa_2 E_l^{(2)*}\right]$ denotes the flux flowing from section $l-1$ to l. At the same time the field amplitudes can be parametrized as $E_{l-1}^{(m)} = a_{l-1}^{(m)} + b_{l-1}^{(m)}$ and $E_l^{(m)} = a_{l-1}^{(m)} e^{\imath k} + b_{l-1}^{(m)} e^{-\imath k}$, where $\omega = 2\cos k$ and k is generally a complex number. The self-consistency requirements impose $E_l^{(m)} \equiv a_{l-1}^{(m)} e^{\imath k} + b_{l-1}^{(m)} e^{-\imath k} = a_l^{(m)} + b_l^{(m)}$, which together with Eq. (12) allows us to calculate the unit TM $\mathcal{T}(\nu)$ such that $\Psi_l = \mathcal{T}(\nu)\Psi_{l-1}$ where $\Psi_l \equiv (a_l^{(1)}, b_l^{(1)}, a_l^{(2)}, b_l^{(2)}, a_l^{(3)}, b_l^{(3)})^T$.

We now analyze numerically the scaling of the modal energy fluxes of the TB model Eq. (12). First we have verified that Eq. (1) is valid for $\mathcal{T}(0)$ using the aforementioned parameters. In Fig. 1c we report our numerical findings for the modal energy flux associated with the slow propagatings S_p and evanescent S_{ev} modes for three different system sizes N. We find that while for $\nu \to 0$ these quantities scale according to the new scaling law Eq. (11), the modal fluxes saturate to a constant value at different $\nu_C \propto 1/N^3$ in accordance to our theoretical prediction, see Eq. (8). In Fig. 1d we report the data for one of the N values referring to a linear-linear plot. We find that $S_{ev}^\mp$, associated with each of the two pairs of evanescent modes (corresponding to the $T^\mp$ blocks in Eq. (2)), balances the divergent of the S_p contribution so that the total flux $S \sim \mathcal{O}(1)$. Finally we have checked numerically the robustness of FMR and of Eq. (11) in the presence of losses and disorder[17,21].

Non-reciprocal layered structures – It is straightforward to reproduce Eqs. (7,8, 11) for finite set-ups with spectral non-reciprocity i.e $\omega(k) \neq \omega(-k)$. Here, instead, we confirm numerically the validity of these equations for the example case of a multilayer periodic magnetic photonic crystal (PC) with proper spatial arrangement, see Fig. 2a[3,6]. We find that the forward slow propagating mode carries an energy flux which scales according to Eq. (11) while the pair of the associated evanescent modes balanced this divergence in a similar manner, see Fig. 2c,d. The remaining (fast) backward propagating mode does not show any flux divergence and has minimal contribution to the total energy flux, see Fig. 2d.

Conclusions - The character of the FMR in finite structures undergoes a transition which is reflected in a change of the scaling behaviour (with detuning ν) of the modal energy flux of the slow propagating modes at critical lengths $L_C \propto 1/\nu^{1/3}$. As opposed to the semi-infinite case, below this length-scale, the energy flux is carried even by (pairs of) evanescent modes. Our results might have important applications to non-reciprocal transport.

[1] P. A. Deymier, Acoustic Metamaterials and Phononic Crystals, (Springer, 2013)

[2] J. D. Joannopoulos, S. G. Johnson, J. N., Winn, & R. D. Meade, *Photonic Crystals: Molding the Flow of Light*, 2nd ed. (Princeton University Press, Princeton, NJ, 2008).

[3] A. Figotin and I. Vitebskiy, Waves Random Complex Me-

dia **16**, 293 (2006).

[4] A. Figotin and I. Vitebskiy. Slow Wave Phenomena in Photonic Crystals (Review article), Laser & Photonic Reviews **5**, 201 (2011).

[5] A. Figotin and I. Vitebskiy, *Electromagnetic Unidirectionality in Magnetic Photonic Crystals*; Book chapter in: Magnetophotonics: From Theory to Applications. Springer Series in Materials Science, 2013.

[6] H. Ramezani, S. Kalish, I. Vitebskiy, and T. Kottos, Phys. Rev. Lett. **112**, 043904 (2014).

[7] A. Figotin, I. Vitebskiy, Phys. Rev. E **63**, 066609 (2001).

[8] A. Figotin, I. Vitebskiy, J. Magn. Mater **300**, 117 (2006)

[9] A. Figotin, I. Vitebskiy, Phys. Rev. E —bf 74, 066613 (2006)

[10] N. Gutman, C. Martijn de Sterke, A. A. Sukhorukov, L. C. Botten, Phys. Rev. A **85**, 033804 (2012).

[11] N. Gutman, W. Hugo Dupree, Y. Sun, A. S. Sukhorukov, C. M. de Sterke, Opt. Express **20**, 3519 (2012).

[12] A. Sukhorukov, A. Lavrinenko, D. Chigrin, D. Pelinovsky, Y. Kivshar, J. Opt. Soc. Am. B **25**, C65 (2008).

[13] W-P Huang, J. Opt. Soc. Am. A **11**, 963 (1994).

[14] T. Kato, *Perturbation theory of linear operators*, Springer (1995).

[15] V. N. Bogaevski and A. Povzner, Algebraic Methods in Nonlinear Perturbation Theory (Springer-Verlag, Berlin, 1991).

[16] P. Lancaster, M. Tismenetsky, *The theory of matrices*, Academic Press (2985).

[17] See Supplemental Material at [URL] for detail explanations.

[18] U. Kuhl, F. Mortessagne, E. Makri, I. Vitebskiy, T. Kottos, submitted (2016).

[19] T. Stegmann, J. A. Franco-Villafane, U. Kuhl, F. Mortessagne, T. H. Seligman, Phys. Rev. B **95**, 035413 (2017).

[20] M. Bellec, U. Kuhl, G. Montambaux, F. Mortessagne, Phys. Rev. B **88**, 115437 (2013).

[21] Z. Ming, H. Li, I. Vitebskiy, T. Kottos, in preparation (2017).